Coumarin as Attractive Casein Kinase 2 (CK2) Inhibitor Scaffold: An Integrate Approach To Elucidate the Putative Binding Motif and Explain Structure–Activity Relationships

Adriana Chilin,[†] Roberto Battistutta,[§] Andrea Bortolato,[†] Giorgio Cozza,[†,‡] Samuele Zanatta,[†] Giorgia Poletto,[‡] Marco Mazzorana,[§] Giuseppe Zagotto,[†] Eugenio Uriarte,[△] Adriano Guiotto,[†] Lorenzo A. Pinna,[‡] Flavio Meggio,[‡] and Stefano Moro*,[†]

Dipartimento di Scienze Farmaceutiche, Università di Padova, via Marzolo 5, Padova, Italy, Dipartimento di Chimica Biologica, Università di Padova, Padova, Italy, Venetian Institute for Molecular Medicine (VIMM) and Dipartimento di Scienze Chimiche, Padova, Italy, and Department of Organic Chemistry Institute of Industrial Pharmacy, Faculty of Pharmacy, University of Santiago de Compostela, Spain

Casein kinase 2 (CK2) is an ubiquitous, essential, and highly pleiotropic protein kinase whose abnormally high constitutive activity is suspected to underlie its pathogenic potential in neoplasia and other diseases. Recently, using different virtual screening approaches, we have identified several novel CK2 inhibitors. In particular, we have discovered that coumarin moiety can be considered an attractive CK2 inhibitor scaffold. In the present work, we have synthetized and tested a small library of coumarins (more than 60), rationalizing the observed structure–activity relationship. Moreover, the most promising inhibitor, 3,8-dibromo-7-hydroxy-4-methylchromen-2-one (DBC), has been also crystallized in complex with CK2, and the experimental binding mode has been used to derive a linear interaction energy (LIE) model.

Introduction

Casein kinase 2 (CK2)[a] is probably the most pleiotropic protein kinase known, with more than 300 protein substrates already recognized, a feature which might, at least partly, account for its lack of strict control over catalytic activity.[1] Its catalytic subunits (α or α′) are in fact constitutively active either with or without the regulatory β-subunits, which appear to play a role in targeting and substrate recruiting, rather than controlling catalytic activity. Although constitutively active CK2 is ubiquitous, essential, and implicated in a wide variety of important cell functions,[2] evidence has been accumulating that its catalytic subunits may behave as oncogenes,[3–6] consistent with the observation that they display an antiapoptotic effect in prostate cancer cell lines.[7] Actually, they are invariably more abundant in tumors compared with normal tissues, and their overexpression causes neoplastic growth in animal and cellular models presenting alterations in the expression of cellular oncogenes or tumor suppressor genes.[8] These data, in conjunction with the observation that many viruses exploit CK2 as phosphorylating agent of proteins essential to their life cycle,[1] are raising interest in CK2 as a potential target for antineoplastic or anti-infectious drugs.[9]

In the last few years, we have performed an intensive screening program, using both conventional and *in silico* approaches, with the aim of discovering novel potent and selective CK2 inhibitors.[10,11] In particular, we have recently
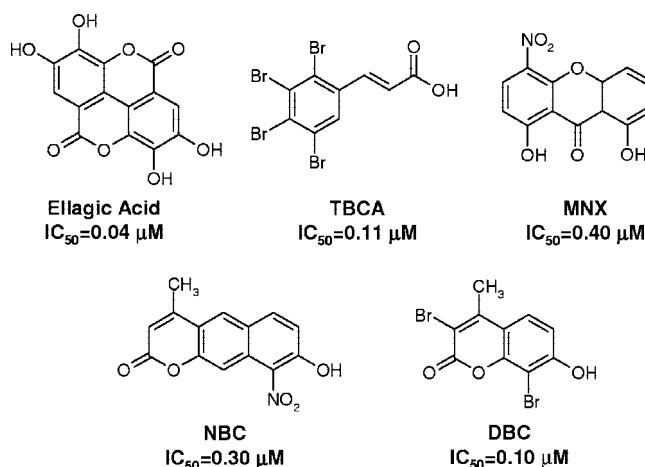

Figure 1. Chemical structures of known CK2 inhibitors.

implemented an in-house molecular database (defined as "MMS-Database") in which almost 2500 kinase inhibitor-like compounds are collected for specific virtual screening applications. Several families of polyphenolic compounds, including a large class of flavones, flavonols, isoflavones, catechins, anthraquinones, coumarins, and tannic acid derivatives, are represented in our molecular database. Following some recent successful reports in discovery of new kinase inhibitors by high-throughput docking of large collections of compounds,[12,13] we have performed a virtual screening experiment targeting the ATP binding site of CK2 by browsing the MMS-database. In this effort, several new derivatives have been reported as potent and selective CK2 inhibitors such as ellagic acid,[14] a naturally occurring tannic acid derivative, tetrabromocinnamic acid (TBCA),[15] 1,8-dihydroxy-4-nitroxanthen-9-one (MNX), 8-hydroxy-4-methyl-9-nitrobenzo[*g*]chromen-2-one (NBC),[10] and 3,8-dibromo-7-hydroxy-4-methylchromen-2-one (DBC),[11] as summarized in Figure 1.

In particular, we focused our attention on the coumarin derivative DBC because coumarins are natural benzopyrone derivatives whose members include also flavonoids. Interest-

---

* To whom correspondence should be addressed. Mailing address: Molecular Modeling Section, Department of Pharmaceutical Sciences, University of Padova, Via Marzolo 5, 35131 Padova, Italy. Tel: +39 049 8275704. Fax: +39 049 827 5366. E-mail: stefano.moro@unipd.it.
† Dipartimento di Scienze Farmaceutiche, Università di Padova.
§ Venetian Institute for Molecular Medicine.
‡ Dipartimento di Chimica Biologica, Università di Padova.
△ University of Santiago de Compostela.
[a] Abbreviations: ASA, accessible surface area; CK2, casein kinase 2; DBC, 3,8-dibromo-7-hydroxy-4-methylchromen-2-one; LIE, linear interaction energy; MMS, molecular modeling section; MNX, 1,8-dihydroxy-4-nitroxanthen-9-one; NBC, 8-hydroxy-4-methyl-9-nitrobenzo[*g*]chromen-2-one; TBCA, tetrabromocinnamic acid; rmsd, root-mean-square deviation; W, water.

ingly, dietary exposure to benzopyrones is quite significant, because these compounds are found in vegetables, fruit, seeds, nuts, coffee, tea, and wine.[16] It is estimated that the average western diet contains approximately 1 g/day of mixed benzopyrones.[16] It is, therefore, not difficult to see why extensive research into their pharmacological and therapeutic properties has been underway over many years.[16,17] In particular, coumarin is a natural substance that has shown antitumor activity *in vivo*, with the effect believed to be due to its metabolites (e.g., 7-hydroxycoumarin).[17] A recent study has shown that 7-hydroxycoumarin inhibits the release of cyclin D1, which is overexpressed in many types of cancer.[17] This knowledge may lead to its use in cancer therapy.

In the present work, we have synthetized and tested a focused library of coumarin derivatives (more than 60) with the aim of elucidating the putative binding motif and explaining structure–activity relationships. In this study, the X-ray diffraction crystal structure of CK2 in complex with DBC has been determined, and it was exploited as a starting point for a linear interaction energy (LIE)[18–25] study to rationalize the different free energies of binding and the key interactions of all coumarin derivatives. This computational approach is an efficient tool to quantitatively explore scaffold decorability and to evaluate regions of the protein active site crucial for ligand binding, as already proven for a class of CK2 inhibitors such as bromo-benzoimidazole.[19]

Results

Focused Coumarin Library. The chemical diversity of our focused coumarin library is reported in Table 1. Several derivatives were unknown until now and they have been newly synthetized as described in the Materials and Methods section. In particular, bromocoumarin derivatives (**19**, **21**, **26**, **31**, **62**, **63**, and **65**) were prepared by direct bromination of coumarin precursors or by appropriate functionalization of bromo-intermediates. Different bromination schemes were used according to starting materials and substitution positions. Bromocoumarins **19** and **21** were synthesized by using *N*-bromosuccinimide in acetonitrile at reflux, while compounds **26**, **31**, **62**, **63**, and **65** were prepared by using bromine in acetic acid at 60 °C.

Iodo or chloro analogs (**2**, **3**, and **22**, respectively) were obtained by direct halogenation at the 8 position of the already brominated coumarins by using iodine and potassium iodide in ammonia solution at room temperature or aluminum chloride at 130 °C.

The acetyl derivative **11** was obtained by esterification of the phenolic function of DBC (**1**) with acetic anhydride and sodium acetate at reflux.

Coumarins carrying a formyl, oxime, or cyano in the 8 position, such as compounds **8**, **12**, and **14**, were prepared starting from the corresponding 3-bromocoumarin. In this way, the 8-coumarinaldehyde **14** was synthesized by formylating the starting coumarin with hexamethylenetetramine in acetic acid at reflux or microwave irradiating at 120 °C, strongly reducing the reaction time and more than doubling the yield in comparison with classical heating. Coumarin **14** was converted to oxime derivative **12** by methanolic hydroxylamine at room temperature, and the oxime group was dehydrated to the cyano group in acetic anhydride at reflux. The 8-cyanocoumarin **8** was also prepared directly by reacting compound **14** with hydroxylamine in *N*-methylpyrrolidone with microwave irradiation at 140 °C.

The 5-bromo derivatives **39** and **40** were synthesized by condensing 2-bromo-6-hydroxybenzaldehyde with diethylmalonate and then hydrolyzing the ethyl ester in alkaline medium.

The piperazinesulfonyl-5-bromo derivatives **43** and **44** were prepared by nucleophilic substitution of the sulfonylchloride intermediates, obtained by reacting the 5-bromocoumarin with chlorosulfonic acid at reflux. The piperazinesulfonyl-8-bromo derivative **45** was obtained in an analogous manner from 8-bromocoumarin.

The remaining compounds (**1**, **4−7**, **9**, **10**, **13**, **15−18**, **20**, **23−25**, **27−30**, **32−38**, **41**, **42**, **46−61**, **64**, **66**, and **67**) were already known and were prepared according to literature methods (see Supporting Information for references). Finally, compounds **41** and **42** were commercially available.

Crystallography. The use of CK2 α subunit from *Zea mays* in cocrystallization experiments has been widely adopted in recent years due to a better stability of the maize enzyme compared with the human CK2. This is also supported by its highly conserved primary structure and by almost identical catalytic properties toward all CK2 inhibitors tested up to now. The crystal structure of the complex between the α catalytic subunit and the β regulatory one of the human protein has been determined,[26] along with that of the isolated α catalytic subunits both from human and from maize.[27–29] From these structures, it emerged that the active site of the human protein is practically identical to that of the maize one (rmCK2). Moreover, it indicates that the formation of the quaternary complex does not influence the conformation of the catalytic subunit, so the latter can be used in design of inhibitors of the holoenzyme. The close sequence and structural similarities between the *Zea mays* and the human α catalytic subunits (which shows 98% sequence identity with the rat one, with all the variations in the extreme C-terminal tail) strongly support the choice to work with the maize enzyme in structural inhibition studies: this enzyme has a higher tendency to produce good diffracting crystals, and this is the reason it has been preferred over the human enzyme.

Like the other inhibitors, DBC binds to CK2 inside the ATP-binding site, in a position similar to those of the anthraquinone MNA[10] and the xanthenone MNX,[10] as shown in Figure 2. The overall structure of the protein is not affected by the binding of the inhibitor. In the final model, 327 residues out of 332 are present, from position 2 to 328; the first methionine and the four C-terminal residues Arg-Thr-Arg-Ala are not visible in the final electron density. The position of the DBC hydroxyl group is almost identical to the analogous function in MNX, lying in an area of positive electrostatic potential near Lys68. This OH group establishes two hydrogen bonds, one with the amine function of the Lys68 side chain and another with a water molecule (W1) that is conserved in all deposited CK2 structures (Figure 2). This H-bonding network seems to have a crucial role in the recognition process of all phenol-like CK2 inhibitors.[30] DBC does not interact directly with the hinge region; the closest atom is the bromine ortho to the carbonyl at 3.7 Å from the Val116 carbonyl.

Linear Interaction Energy Model. A linear interaction energy (LIE) approach has been used to evaluate the binding free energy of this class of CK2 inhibitors following a computational approached recently proposed by our laboratory.[19] It was possible to include a total of 16 coumarins shown in Table 1 in the training set to generate the quantitative LIE model (Table 2).

Most probably this is linked to the fact that some particular chemical features, present only in this subset of molecules, are the key to achieve a DBC-like binding mode, which was used as starting point for the LIE calculation. First of all, a hydroxyl group capable of interacting with the conserved water W1 (see Figure 2) must be present at the 7 position of the coumarin scaffold. This is the only crucial electrostatic interaction shown by this class of

Table 1. Inhibition of CK2 by Coumarin Analogues[a]
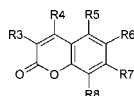
Name	R3	R4	R5	R6	R7	R8	IC$_{50}$ (μM)	ΔG_{exp} (kcal/mol)	Predicted pKa[a]	Ionic State
1 DBC	-Br	-CH$_3$	-H	-H	-OH	-Br	0.10 (K$_i$=0.06 μM)	-9.61	5.88	-1
2	-Br	-CH$_3$	-H	-H	-OH	-I	0.28	-9.00	5.96	-1
3	-Br	-CH$_3$	-H	-H	-OH	-Cl	0.32	-8.92	5.94	-1
4	-Br	-CH$_3$	-H	-Br	-OH	-H	0.66	-8.48	5.88	-1
5	-H	-CH$_3$	-H	-H	-OH	-Br	0.74	-8.42	6.48	-1
6	-H	-CH$_3$	-H	-H	-OH	-I	0.80	-8.37	6.56	-1
7	-Br	-CH$_3$	-H	-Br	-OH	-Br	1.90	-7.85	4.35	-1
8	-Br	-CH$_3$	-H	-H	-OH	-CN	1.90	-7.85	4.62	-1
9	-Br	-CH$_3$	-H	-OH	-OH	-Br	2.00	-7.82	5.72	-1
10	-H	-CH$_3$	-H	-H	-OH	-Cl	2.20	-7.77	6.54	-1
11	-Br	-CH$_3$	-H	-H	-OCOCH$_3$	-Br	2.50	-7.69	/	0
12	-Br	-CH$_3$	-H	-H	-OH	-CH=NOH	2.50	-7.69	6.53	-1
13	-H	-CH$_3$	-H	-I	-OH	-I	2.66	-7.65	5.12	-1
14	-Br	-CH$_3$	-H	-H	-OH	-COH	3.30	-7.52	5.62	-1
15	-Br	-CH$_3$	-H	-NO$_2$	-OH	-H	3.30	-7.52	4.20	-1
16	-Br	-CH$_3$	-H	-Br	-OH	-OH	3.60	-7.47	5.72	-1
17	-H	-CH$_3$	-H	-H	-OH	-NO$_2$	4.00	-7.41	2.95	-1
18	-H	-CH$_2$Cl	-H	-H	-OH	-OH	4.00	-7.41	7.44	0
19	-Br	-CH$_3$	-H	-Br	-OH	-NO$_2$	4.00	-7.41	0.59	-1
20	-Br	-CH$_3$	-H	-H	-OH	-NO$_2$	4.00	-7.41	2.35	-1
21	-Br	-CH$_3$	-H	-NO$_2$	-OH	-Br	4.00	-7.41	2.42	-1
22	-Br	-CH$_3$	-H	-Br	-OH	-Cl	4.03	-7.41	4.41	-1
23	-H	-CH$_3$	-H	-H	-OH	-CN	4.20	-7.38	5.22	-1
24	-Br	-CH$_3$	-H	-H	-OH	-OH	10.50	-6.83	9.99	0
25	-H	-H	-H	-H	-OH	-Cl	10.70	-6.82	6.43	-1
26	-Br	-H	-H	-Br	-OH	-Br	15.21	-6.61	4.24	-1
27	-H	-CH$_3$	-H	-H	-OH	-C=NOH	20.00	-6.45	7.13	0
28	-Br	-CH$_3$	-OH	-Br	-OH	-Br	21.50	-6.41	4.14	-2
29	-H	-CH$_3$	-H	-H	-OH	[structure]	22.70	-6.37	5.36	-1
30	-CH$_3$	-CH$_3$	-H	-H	-OH	-OCH$_3$	27.00	-6.27	8.13	0
31	-Br	-OH	-H	-H	-OH	-Br	28.00	-6.25	6.49	-2
32	-H	-CH$_3$	-H	-NO$_2$	-OH	-CH$_3$	30.00	-6.21	5.19	-1
33	-H	-CH$_3$	-H	-NO$_2$	-OH	-H	30.00	-6.21	4.80	-1
34	-Br	-CH$_3$	-H	-OH	-OH	-H	31.00	-6.19	7.25	0
35	-H	-H	-OH	-H	-OH	-H	34.96	-6.12	8.61	0
36	-H	-CH$_3$	-OH	-H	-OH	-H	34.96	-6.12	8.72	0
37	-Br	-H	-H	-NO$_2$	-OH	-CH$_3$	35.00	-6.12	4.48	-1
38	-Br	-OH	-H	-H	-OH	-H	39.00	-6.05	7.4	0
39	-COOEt	-H	-Br	-H	-H	-H	117.5	-5.39	/	0
40	-COO$^-$	-H	-Br	-H	-H	-H	147.00	-5.26	/	-1
41	-H	-CH$_3$	-H	-H	-OH	-H	>100.00	>-5.50	8.00	0
42	-H	-H	-H	-H	-OH	-H	>100.00	>-5.50	7.89	0
43	-H	-H	-Br	-H	-OH	[structure]	>100.00	>-5.50	3.78	-1
44	-H	-H	-Br	[structure]	-H	-H	>100.00	>5.50	/	0
45	-H	-H	-H	[structure]	-H	-Br	>100.00	>-5.50	/	0
46	-NO$_2$	-CH$_3$	-H	-NO$_2$	-OH	-H	>100.00	>5.50	4.36	-1
47	-H	-CH$_3$	-H	-NO$_2$	-OH	-OH	>100.00	>-5.50	4.61	-1
48	-NO$_2$	-CH$_3$	-H	-H	-H	-H	>100.00	>-5.50	/	-1
49	-NO$_2$	-CH$_3$	-H	-NO$_2$	-OH	-CH$_3$	>40	>-6.00	4.77	-1
50	-H	-CH$_3$	-H	-H	-OH	-OCH$_3$	>40	>-6.00	8.02	0
51	-H	-CH$_2$Cl	-H	-H	-OH	-OCH$_3$	>40	>-6.00	7.74	0
52	-CH$_3$	-H	-OCH$_3$	-H	-OH	-H	>40	>-6.00	7.64	0
53	-H	-CH$_2$OH	-H	-H	-OH	-OH	>40	>-6.00	10.48	0
54	-NO$_2$	-CH$_3$	-H	-NO$_2$	-OH	-NO$_2$	>100.00	>5.50	0.71	-1
55	-H	-CH$_3$	-H	-NO$_2$	-OCOCH$_3$	-H	>100.00	>5.50	/	0
56	-H	-CH3	-H	-H	-OCOCH$_3$	-NO$_2$	>100.00	>-5.50	/	0
57	-H	-H	-H	[structure]	-OH	-OCH$_3$	>100.00	>-5.50	6.64	-1
58	-H	-H	-H	[structure]	-OH	-OCH$_3$	>100.00	>5.50	5.54	-1
59	-H	-CH$_2$OH	-H	-H	-OH	-H	>40	>-6.00	7.89	0
60	-H	-CH$_2$Cl	-H	-H	-OH	-H	>40	>-6.00	7.72	0
61	-NH$_2$	-H	-H	-H	-OH	-OCH$_3$	>40	>-6.00	8.16	0
62	-Br	-CH$_3$	-H	-H	-NH$_2$	-Br	>40	>-6.00	/	0
63	-Br	-CH$_3$	-H	-Br	-NH$_2$	-Br	>40	>-6.00	/	0
64	-H	-CH$_3$	-H	-H	-OH	-COH	>40	>-6.00	6.22	-1
65	-Br	-OH	-H	-Br	-OH	-Br	>40	>-6.00	4.49	-2
66	-Br	-CH$_3$	-H	-Br	-OCH$_3$	-H	>40	>-6.00	/	0
67	-Br	-CH$_3$	-H	-H	-OCH$_3$	-Br	>40	>-6.00	/	0

[a] The IC$_{50}$ activity data represent the means of three independent experiments with SEM never exceeding 15%. The *in silico* prediction of R7 substituent pKa and the net charge of the most populated ionic state at physiological pH are shown. [b] The error estimated on the predicted pKa of the phenolic OH at position 7 is ±0.02.
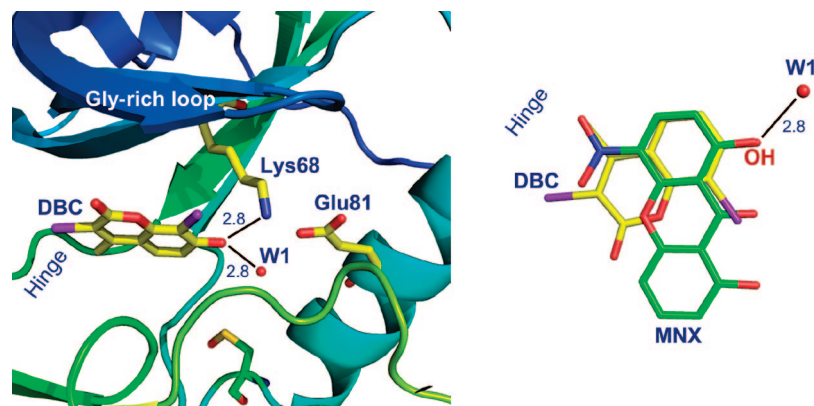
Figure 2. The top panels shows DBC bound to the CK2 ATP binding site. The hydroxyl function is involved in two hydrogen bonds (at a distance of 2.8 Å) with Lys68 and the conserved water molecule W1. The top panel shows a superimposition of the two inhibitors DBC (yellow carbon atoms) and MNX (green carbon atoms). Bromine atoms are shown in magenta. Note the identical position of the OH function of DBC and MNX. As reference, water molecule W1 and the zone of the hinge region are indicated.

Table 2. Ensemble Average LIE Energy Terms for the Inhibitors Used To Build the Energy Model[a]

name	U_{elect}^{b-f} (kcal/mol)	U_{vdw}^{b-f} (kcal/mol)	HASA^{b-f} (kcal/mol)	ASA^{b-f} (kcal/mol)	ASA+$^{b-f}$ (kcal/mol)	ASA−$^{b-f}$ (kcal/mol)	CASA+$^{b-f}$ (kcal/mol)	CASA−$^{b-f}$ (kcal/mol)	VSA^{b-f} (kcal/mol)	PASA^{b-f} (kcal/mol)
1 DBC	−197.7653	1.5702	−448.1037	−557.2585	−100.0504	−288.9721	−74.2579	868.0718	2806.5571	−109.1548
2	−193.7874	4.4171	−451.7560	−564.7581	−100.9600	−294.8176	−76.9676	−187.3542	2543.4438	−113.0021
3	−215.5250	1.5011	−430.4421	−540.7503	−100.0653	−273.8589	−59.2773	2885.0308	1206.3640	−110.3082
4	−220.7834	18.9818	−447.4083	−557.1554	−89.2716	−303.8774	−103.1900	4220.9419	−1929.1779	−109.7472
5	−167.8966	2.2074	−397.6865	−512.5418	−113.6143	−233.5788	−64.8164	4264.6226	2366.2527	−114.8553
6	−169.0103	5.0361	−398.7990	−516.8976	−113.9363	−237.4862	−66.6977	3336.0249	2459.3225	−118.0987
8	−219.6383	−0.4217	−374.5649	−553.6124	−126.7920	−260.2887	−60.4464	4194.0859	2781.6345	−179.0476
9	−231.1221	4.3391	−414.0914	−570.3610	−109.6718	−292.0350	−89.8760	2417.8528	3626.5566	−156.2696
10	−182.6900	3.4665	−379.5748	−494.7814	−113.7104	−217.3335	−50.6239	6509.5933	962.4318	−115.2067
12	−229.2684	13.3805	−381.2005	−574.2347	−160.1861	−248.5138	−88.1841	7457.0674	−1039.3051	−193.0342
14	−212.7549	2.0311	−388.4405	−543.1951	−145.6445	−230.2745	−61.6509	3919.6196	5357.7446	−154.7546
17	−192.0742	3.4807	−373.1952	−560.5029	−101.5250	−291.5494	−66.2913	5628.3013	4908.8560	−187.3077
20	−197.6469	6.5256	−319.2815	−513.6910	−112.6414	−237.0944	−56.6301	9666.1660	3728.5420	−194.4096
23	−218.6269	3.7350	−320.2022	−503.8472	−139.2490	−199.9986	−52.0343	8096.2407	3481.0146	−183.6451
25	−191.6230	3.6139	−356.0089	−70.6675	−122.9562	−235.5503	−46.7456	6553.1392	1366.0836	−114.6586
27	−202.7459	12.6623	−332.0560	−528.6724	−173.7345	−192.0848	−78.5291	10961.5870	−1002.8069	−196.6165

[a] U_{elect}^{b-f}, U_{vdw}^{b-f}, HASA^{b-f}, ASA^{b-f}, ASA+$^{b-f}$, ASA−$^{b-f}$, CASA+$^{b-f}$, CASA−$^{b-f}$, VSA^{b-f}, and PASA^{b-f} are, respectively, electrostatic, van der Waals, total hydrophobic surface area, water accessible surface area, positive accessible surface area, negative accessible surface area, charge-weighted positive surface area, charge-weighted negative surface area, van der Waals surface area, and total polar surface area energy terms. All the energy terms are the result of the subtraction from the bound state energy estimation of the free state energy estimation. Together with U_{elect}^{b-f} and U_{vdw}^{b-f}, the HASA^{b-f} surface has been chosen to build the final energy model.

inhibitors, and it seems to be strongly modulated in its intensity by the presence of an electron-withdrawing substituent at the 6 position of the coumarin scaffold. According to the Hammett theory, the presence of an electron-withdrawing substituent in the ortho position to phenol OH increases the acidic behavior of the phenolic group. To simulate this highly polarized hydrogen bonding, we created two possible working hypothesis: (I) in the first case, the hydroxyl group in 7 becomes anionic before forming the complex with CK2, and it is considered with a formal net charge equal to −1; (II) in the second assumption, phenol OH participates at the active site in its neutral form, and the hydrogen bonding with water W1 is so highly polarized that can be more suitably modeled as an ionic couple between a hydronium ion (water W1 is transformed into H_3O^+) and the anionic form of the phenol OH (Figure 2). Both these possibilities are in accordance with the fact that only ligands with a low pK_a, estimated using the ACDLabs[31] package, can be studied using the LIE approach considering a DBC-like binding mode. Both hypotheses resulted in high-quality and roughly comparable energy models, the best one presented here is derived by *in situ* ionic couple theory. Finally, almost all possess hydrophobic groups at the 8 position of the coumarin moiety, a hydrogen atom in position 5, and a nonhydrophobic group at the 6 position.

The calculated energy terms (Table 2) result in a final model with $\alpha = 0.029$, $\beta = -0.003$, and $\gamma = 0.016$. The obtained correlation factor is $r^2 = 0.771$ with a rmsd of 0.303 kcal/mol, and the cross-validated q^2 is slightly lower ($q^2 = 0.633$, cross-validated rmsd = 0.491 kcal/mol). Free energies of binding, calculated from experimental IC_{50}[19] and predicted ΔG_{bind} are shown in Table 3 and finally plotted in Chart 1.

Discussion

Qualitative Structure–Activity Relationship (SAR). Several important structural features of coumarin derivatives can be identified from a first qualitative analysis of their activity on CK2 (Table 1). Primarily, the hydroxyl group at the 7 position of the coumarin moiety can be considered an essential feature even if not sufficient to achieve an IC_{50} in a submicromolar range. Indeed, to increase the inhibitory potency, an electron-withdrawing substituent should be simultaneously present at position 8. For instance, in derivative **5** ($IC_{50} = 0.74\ \mu M$), a simple substitution of the bromide atom with a methoxy group (derivative **50**) results in a complete loss of activity. This important effect can be rationalized according to the increase of the acidity of the 7-hydroxyl group as confirmed by our *in silico* predictions, where to achieve a submicromolar activity,

Table 3. Comparison of Experimental (ΔG_{exp}, kcal/mol), Predicted (ΔG_{pred}, kcal/mol) and Cross-Validated (ΔG_{cv}, kcal/mol) Free Energies of Binding for the 16 Inhibitors Included in the Model

name	ΔG_{exp} (kcal/mol)	ΔG_{pred} (kcal/mol)	ΔG_{cv} (kcal/mol)
1 DBC	−9.61	−9.04	−8.87
2	−9.00	−9.03	−9.04
3	−8.92	−8.69	−8.63
4	−8.48	−8.44	−8.37
5	−8.42	−8.30	−8.25
6	−8.37	−8.23	−8.18
8	−7.85	−7.82	−7.81
9	−7.82	−8.29	−8.45
10	−7.77	−7.92	−7.94
12	−7.69	−7.49	−7.41
14	−7.52	−8.00	−8.07
17	−7.41	−7.78	−7.82
20	−7.41	−6.79	−6.59
23	−7.38	−6.81	−6.57
25	−6.82	−7.50	−7.59
27	−6.45	−6.80	−6.97

it is necessary that the pK_a of the 7-hydroxyl group is lower than 7. This hypothesis is also supported by the experimental evidence that the substitution on DBC of the 7-hydroxyl group with the 7-amine group results again in a complete loss of activity (see derivative **62**).

Hydrophobic groups at positions 3 and 4, such as bromide or methyl, improve the activity, while substitutions at the 5 position result in a loss of inhibition efficiency. Halogen or nitro substituents at position 6 can be compatible with an activity around 1–4 μM according to the other decorations of coumarin moiety.

SAR Considering DBC−CK2 Complex Structural Information. The crystal structure of DBC in complex with CK2 nicely explains the pharmacophore derived by SAR considerations, as summarized in Figure 3.

In fact, hydrophobic groups in positions 3, 4, and 8 can interact through van der Waals interactions with the CK2 active site, while the importance of the 7-hydroxyl group is explained by its key interactions with Lys68 and water W1, a water molecule very well conserved in all CK2−inhibitor complexes available. These represent the only electrostatic interactions exploited by DBC in the binding to CK2, and most probably all other coumarin derivatives must possess this ionizable hydroxyl group to achieve a similar binding mode.

However, considering the strong hydrophobic nature of the CK2 ATP-binding pocket, the crucial role of both hydrophobic interactions and desolvation effects in ligand binding is doubtless. It is most likely that when the hydrophobic contribution to the binding becomes sufficiently strong, it is possible to have active compounds that could present a binding mode different from DBC as seen for the dibromobenzo imidazole and triazole derivatives.[19] In fact, crystal structure analysis and molecular modeling studies have demonstrated that these scaffolds can bind the CK2 active pocket into two different orientations. When the inhibitor can interact through a polarized hydrogen bonding with the water molecule, like tetrabromobenzotriazole (TBB) derivatives, the position of the planar aromatic scaffold is similar to the one presented by the DBC−CK2 crystal structure; in contrast, the ligand can be shifted and rotated nearer the hinge region, like already observed in K44, K37, K25, or K17 crystal structures.[32] In other words, even if DBC and TBB present different chemical structures, their ATP-binding pocket recognitions are comparable, and water molecules seem to adapt the protein to the ligand peculiarities.

Quantitative Free Energy of Binding Model. Starting from these qualitative considerations, we analyzed the structure–activity

relationship of coumarin derivatives from a more quantitative point of view. Using the linear interaction energy method, it has been possible to build up a quantitative model using 16 coumarin derivatives and including in this training set all submicromolar inhibitors (Figure 3). The final model is statistically acceptable.
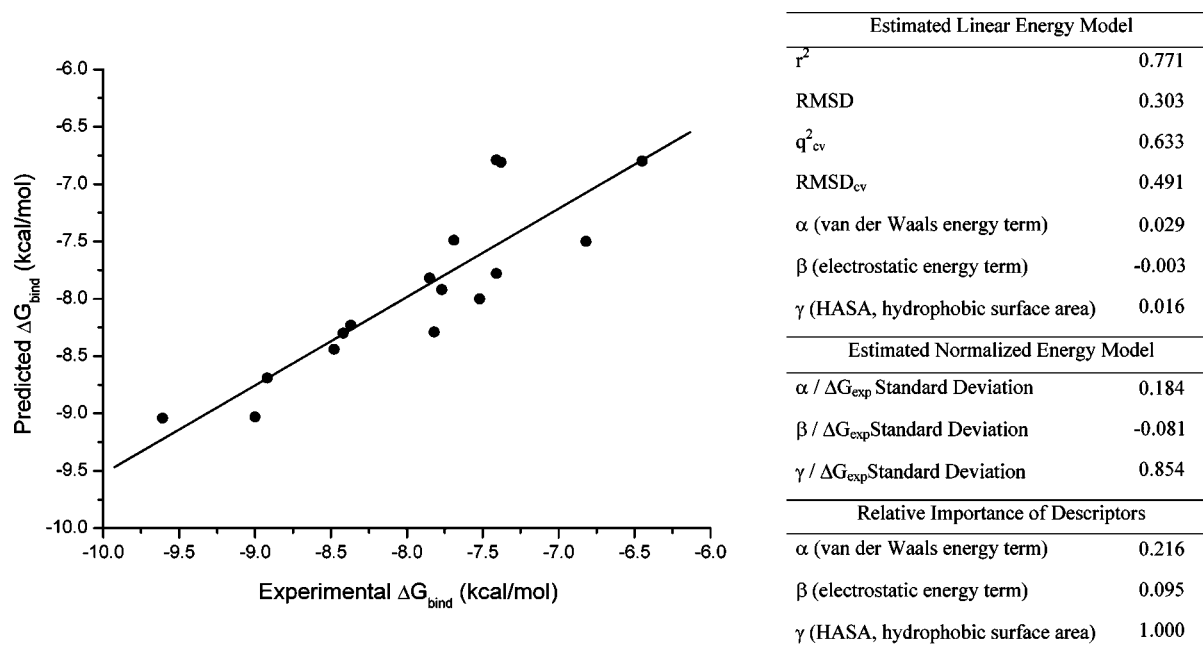
This computational technique allows us to evaluate the principal contributions for inhibitor activity. The strongest effect results from van der Waals interactions ($\alpha = 0.029$), in agreement with the steric complementarily between the CK2 active pocket and almost all coumarin derivatives studied. This is followed in absolute importance by the hydrophobic effect ($\gamma = 0.016$), constituting the most variable part among the test set. Indeed this aspect is the most important to discriminate the relative activity of coumarins studied, as shown by the γ normalized value of 0.854. In contrast, the very low absolute weight of the electrostatic contribution ($\beta = -0.003$) is linked to the fact that the strong interaction with water molecule W1 is common in all inhibitors. For this reason, even if this interaction is crucial for the inhibitor orientation in the active pocket, it is not important to discriminate the activity difference inside the series studied.

In particular, the nonpolar contribution to the free energy of solvation in a LIE study is represented by the difference between the solvent-accessible surface area of the ligand in complex and that of the ligand free in solution (ASA^{b-f}). Since this contribution seems crucial for the binding of CK2 inhibitors,[2,28] we tried to include it in our LIE model also using alternative types of solvent-accessible surface, such as the positive and negative accessible surface area (respectively, $ASA+^{b-f}$ and $ASA-^{b-f}$), the charge-weighted positive and negative surface area (respectively, $CASA+^{b-f}$ and $CASA-^{b-f}$), the van der Waals surface area (VSA^{b-f}), the total polar surface area ($PASA^{b-f}$), and the total hydrophobic surface area ($HASA^{b-f}$) as collected in Table 2. Interestingly, using only the total hydrophobic surface area ($HASA^{b-f}$), it is possible to obtain an acceptable LIE model, pointing out the important role of the hydrophobic contribution in the final free energy of binding. This is a clear indication of the major role played by the several nonpolar amino acid side chains that characterize the CK2 active pocket.

The final energy model derived was able to predict almost all inhibitors with a hydrophobic group at the 8 position and with the pK_a value of the 7-hydroxyl group lower than 7 units. A possible reason can be related to the peculiarity of CK2 ATP binding site to allow different binding modes, even among similar inhibitors, as demonstrated by several structural data available. Indeed these chemical−physical requisites of coumarins seem to discriminate between a DBC-like binding mode, used as starting point for the LIE study, and other possible ligand orientations.

Conclusion

A CK2 inhibitor design strategy that started more than 15 years ago with the first ribofuranosyl-benzimidazole derivatives[33] has been continuously evolving with a progressive development of many submicromolar inhibitors, constantly improving the structural knowledge of their activity. Results presented here can be considered a new important tessera in the always more complete CK2 mosaic. The multidisciplinary approach used in this work connects in a virtual circle chemical synthesis, biological assays, structural information, and different molecular modeling techniques to rationally design new CK2 inhibitors. More than 60 coumarin derivatives synthesized and tested represent a strong base to analyze, propose, and corroborate hypotheses about essential inhibitor features for CK2 binding. In this particular effort, the crystallization of the DBC−CK2 complex represents a very

Chart 1. Free Energy of Binding Estimated by the LIE Model of Each Inhibitor Used versus the Experimentally Measured Data[a]

Estimated Linear Energy Model	
r^2	0.771
RMSD	0.303
q^2_{cv}	0.633
RMSD$_{cv}$	0.491
α (van der Waals energy term)	0.029
β (electrostatic energy term)	-0.003
γ (HASA, hydrophobic surface area)	0.016
Estimated Normalized Energy Model	
α / ΔG$_{exp}$ Standard Deviation	0.184
β / ΔG$_{exp}$ Standard Deviation	-0.081
γ / ΔG$_{exp}$ Standard Deviation	0.854
Relative Importance of Descriptors	
α (van der Waals energy term)	0.216
β (electrostatic energy term)	0.095
γ (HASA, hydrophobic surface area)	1.000

[a] On the bottom, the correlation coefficient (r^2) and cross-validated coefficient (q^2) are shown. For the whole set, rmsd and cross-validated rmsd (rmsd$_{cv}$) were calculated. α, β, and γ are the resulting coefficients of the LIE equation for CK2 score.
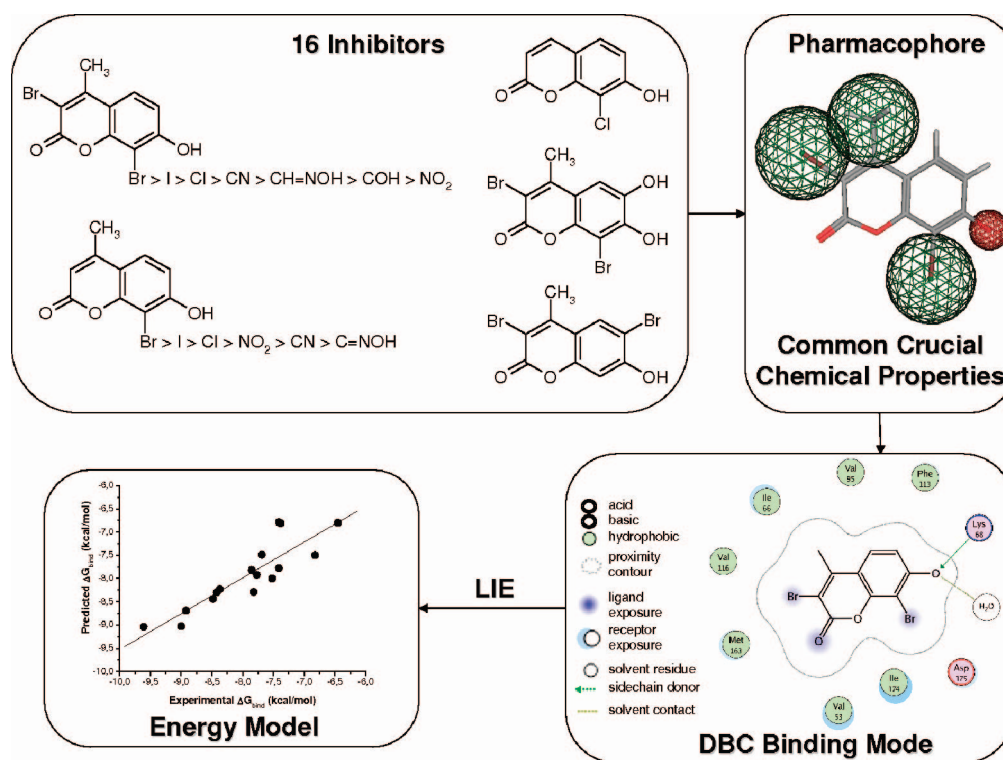
Figure 3. The 16 inhibitors used to build the LIE energy model using the DBC binding mode as starting position for the computational study are shown in the upper left. The more the scaffold satisfies the base pharmacophore shown on the upper right (the green spheres represent hydrophobic molecular regions, the small red region stands for a strongly polarized hydrogen bonding donor), the higher is the probably that it will possess the chemical features to achieve a DBC similar binding mode in the CK2 ATP binding pocket.

important improvement in mapping the most crucial chemical features into CK2 recognition processes. Full understanding of principal binding features is the first step in the inhibitor design process based on biostructural information. Finally, starting from this new crystallographic information, a linear interaction energy method has been used as an efficient computational approach to understand the importance of different energy contributions to the final free energy of binding.

Materials and Methods

Chemistry. All the details about synthetic methods and analytical and spectral data for the newly synthesized compounds are

Table 4

Data Collection Statistics[a]	
data collection wavelength (Å)	0.979 709
space group	*C*2
a, *b*, *c* (Å)	141.68, 60.25, 44.90
α, β, γ (deg)	90.0, 103.0, 90.0
solvent content	49%
max resolution (Å)	1.84 (1.84−1.94)
independent reflns	27 834 (2671)
multiplicity	3.2 (1.5)
$\langle 1/\sigma \rangle$	9.8 (1.5)
R_{merge} (%)	5.7 (32.9)
completeness (%)	86.5 (57.4)

Final Model Statistics	
protein atoms	2729
protein residues	327
water molecules	218
R/R_{free}	21.4/26.8
overall mean *B* value (Å^2)	28.0
Ramachandran plot statistics (MolProbity validation)[37]	
residues in favored regions	98%
residues in allowed regions	100%
rms on distances (Å)	0.011
rms on angles (deg)	1.27

[a] Numbers in parentheses refer to the highest resolution bin (1.84–1.94 Å).

described in Supporting Information. For the already known compounds whose ^{1}H NMR and HRMS data were not yet available in the literature, these data are reported in Supporting Information, together with elemental analyses.

Crystal Preparation of Maize CK2α in Complex with DBC and Data Collection. The recombinant CK2 α-subunit from *Zea mays* was expressed in *Escherichia coli*, isolated, and purified according to a previously described method.[34] Crystals of the CK2 complex with the inhibitor DBC were obtained by cocrystallization with the sitting drop vapor diffusion technique. A 25 mM inhibitor solution (100% DMSO) was added to the 8 mg/mL protein stock solution in the proper amount to have an inhibitor−protein molar ratio of 3 to 1 and not to exceed a 5% DMSO concentration in the final protein solution. Each solution was diluted with 2 volumes of water and allowed to stand for 2 h in ice. Crystallization drops were obtained by mixing a 3 μL drop of preincubated protein−inhibitor solution with 1 μL of precipitant solution (10–20% PEG 4000, 0.2 M sodium acetate, 0.1 M Tris, pH 8). Each drop was equilibrated against 500 μL of the same precipitant solution (20% PEG 4000). Crystals grew in a few days at 293 K.

X-ray diffraction data were collected at ESRF beamline BM30A in Grenoble at a temperature of 100 K. Before mounting, crystals were cryoprotected by a very rapid soaking in type B immersion oil (Hampton Research, Aliso Viejo, CA). Data were indexed with MOSFLM[35] and then scaled with SCALA from the CCP4 software package.[36]

Structure Determination and Refinement. The CK2−DBC complex crystallizes in space group *C*2, with one molecule in the asymmetric unit. To find the best position inside the unit cell, an initial rigid body transformation on the model of the apoenzyme was adequate, using the rigid body refinement option of REFMAC 5 (CCP4 suite).[36] The refinement was carried out using REFMAC5. Data collection and final model statistics are reported in Table 4. The presence of the inhibitors in the active site was clear since the beginning of the refinement in both $F_o - F_c$ and $2F_o - F_c$ maps. The definition files for the inhibitor were created using the monomer library sketcher routine of CCP4. Refinement was carried out by alternating automated cycles and manual inspection steps using the graphic program Coot v.0.2.[38] The stereochemistry and geometric properties of the final model were checked using Coot validate analysis and Sfcheck and Procheck in CCP4 suite and were adequate for the resolution.

Data Deposition. The coordinates for the model of CK2 in complex with DBC has been deposited at the RCSB Protein Data Bank with ID code 2QC6.

Phosphorylation Assay. Native CK2 was purified from rat liver, as previously described.[39] CK2 phosphorylation assays was carried out at 37 °C in the presence of increasing amounts of each inhibitor in a final volume of 25 μL containing 50 mM, Tris-HCl (pH 7.5), 100 mM NaCl, 12 mM MgCl$_2$, and 0.02 mM [^{33}P]-ATP (500–1000 cpm/pmol), unless otherwise indicated. The phosphorylatable substrates were the synthetic peptide substrate RRRADDSDDDDD (100 μM). Reaction started with the addition of the kinase and was stopped after 10 min by addition of 5 μL of 0.5 M orthophosphoric acid before spotting aliquots onto phosphocellulose filters. Filters were washed in 75 mM phosphoric acid (5–10 mL each) four times and then once in methanol and dried before counting.[40] Each determination was repeated in three independent experiments, and the means of the resulting values were calculated.

Protein and Inhibitors Preparation. Using the software package Molecular Operating Environment (MOE 2006.08),[41] all the ligands and the X-ray diffraction crystal structure of CK2 in complex with the ATP competitive inhibitor DBC were prepared for the linear interaction energy analysis. The water W1 was included in the protein active site for the molecular modeling study. This molecule indeed is well-conserved in almost all CK2−inhibitor complex crystal structures and seems crucial for their binding. Hydrogens were added and energy minimized using the AMBER99 force field[42] until the energy gradient reached 0.05 kcal/mol. This protocol was exploited for both the neutral and anionic states of DBC to achieve two possible orientations of the water as donor or acceptor of hydrogen bonding. Furthermore, to fully understand the importance of acidity of the 7-hydroxy coumarin derivatives, the hypothesis of the ionic couple formation in the active site created by the anionic DBC form and the hydronium ion has been investigated. All inhibitors were built with MOE[9] and energy minimized using the MMFF94x force field[43] until a 0.01 energy gradient was attained. Their ionic states were evaluated using ACDLabs suite,[32] and as starting pose of the LIE calculation, the molecules were superimposed to DBC, since all these ligands have a similar scaffold and it is likely that they share a common binding mode.

Linear Interaction Energy Method Calculation. The LIE method is based on two different simulations, one describing the molecule free in solution (U^f) and the other considering the ligand−protein complex (U^b). In this approach, the inhibitor free energy of binding to a macromolecule is considered to be linearly correlated to several energy terms calculated using a molecular mechanics force field[1] as shown in the following formula:

$$\Delta G_{\text{bind}} = \alpha(\langle U_{\text{vdw}}^b \rangle - \langle U_{\text{vdw}}^f \rangle) + \beta(\langle U_{\text{elec}}^b \rangle - \langle U_{\text{elec}}^f \rangle) + \gamma(\langle U_{\text{cav}}^b \rangle - \langle U_{\text{cav}}^f \rangle) \quad (1)$$

Brackets indicate that the ensemble average of the energy values of van der Waals interactions (U_{vdw}), electrostatic contributions (U_{elec}), and the cavity parameter (U_{cav})[44] are considered during the simulation. Using a training set of molecules with known activity, we built a semiempirical energy model by fitting the three different parameter coefficients (α, β, and γ) to the free energy of binding.[19]

The LIE energy model was created using the default options of the MOE-LIE suite.[41] Briefly, using the MMFF94x force field and the surface generalized Born (SGB) implicit solvent,[45] we performed a Truncated Newton minimization for ligands in complex with CK2 and free in solution with a residue-based cutoff distance of 15 Å, a 0.5 root-mean-square (rms) gradient for convergence, and a maximum of 500 steps. The energy terms calculated with this protocol were used to build the binding free energy model.

Supporting Information Available: Experimental procedures and spectral data of all newly synthesized compounds and ^{1}H NMR and HRMS data of some already known compounds. This material is available free of charge via the Internet at http://pubs.acs.org.

References

(1) Meggio, F.; Pinna, L. A. One-thousand-and-one substrates of protein kinase CK2? *FASEB J.* **2003**, *17*, 349–368.

(2) Litchfield, D. W. Protein kinase CK2: Structure, regulation and role in cellular decisions of life and death. *Biochem. J.* **2003**, *369*, 1–15.

(3) Seldin, D. C.; Leder, P. Casein kinase II alpha transgene-induced murine lymphoma: relation to theileriosis in cattle. *Science* **1995**, *267*, 894–897.

(4) Kelliher, M. A.; Seldin, D. C.; Leder, P. Tal-1 induces T cell acute lymphoblastic leukemia accelerated by casein kinase IIα. *EMBO J.* **1996**, *15*, 5160–5166.

(5) Landesman-Bollag, E.; Channavajhala, P. L.; Cardiff, R. D.; Seldin, D. C. p53 deficiency and misexpression of protein kinase CK2α collaborate in the development of thymic lymphomas in mice. *Oncogene* **1998**, *16*, 2965–2974.

(6) Orlandini, M.; Semplici, F.; Ferruzzi, R.; Meggio, F.; Pinna, L. A.; Oliviero, S. Protein kinase CK2α is induced by serum as a delayed early gene and cooperates with Ha-ras in fibroblast transformation. *J. Biol. Chem.* **1998**, *273*, 21291–21297.

(7) Guo, C.; Yu, S.; Wang, H.; Davis, A. T.; Green, J. E.; Ahmed, K. A potential role of nuclear matrix-associated protein kinase CK2 in protection against drug-induced apoptosis in cancer cells. *J. Biol. Chem.* **2001**, *276*, 5992–5999.

(8) Tawfic, S.; Yu, S.; Wang, H.; Faust, R.; Davis, A.; Ahmed, K. Protein kinase CK2 signal in neoplasia. *Histol. Histopathol.* **2001**, *16*, 573–582.

(9) Unger, G. M.; Davis, A. T.; Slaton, J. W.; Ahmed, K. Protein kinase CK2 as regulator of cell survival: implications for cancer therapy. *Curr. Cancer Drug. Targets* **2004**, *4*, 77–84.

(10) De Moliner, E.; Moro, S.; Sarno, S.; Zagotto, G.; Zanotti, G.; Pinna, L. A.; Battistutta, R. Inhibition of protein kinase CK2 by anthraquinone-related compounds. A structural insight. *J. Biol. Chem.* **2003**, *278*, 1831–1836.

(11) Meggio, F.; Pagano, M. A.; Moro, S.; Zagotto, G.; Ruzzene, M.; Sarno, S.; Cozza, G.; Bain, J.; Elliott, M.; Deana, A. D.; Brunati, A. M.; Pinna, L. A. Inhibition of protein kinase CK2 by condensed polyphenolic derivatives. An in vitro and in vivo study. *Biochemistry* **2004**, *43*, 12931–12936.

(12) Vangrevelinghe, E.; Zimmermann, K.; Schoepfer, J.; Portmann, R.; Fabbro, D.; Furet, P. Discovery of a potent and selective protein kinase CK2 inhibitor by high-throughput docking. *J. Med. Chem.* **2003**, *46*, 2656–2662.

(13) Toledo-Sherman, L.; Deretey, E.; Slon-Usakiewicz, J. J.; Ng, W.; Dai, J. R.; Foster, J. E.; Redden, P. R.; Uger, M. D.; Liao, L. C.; Pasternak, A.; Reid, N. Frontal affinity chromatography with MS detection of EphB2 tyrosine kinase receptor. 2. Identification of small-molecule inhibitors via coupling with virtual screening. *J. Med. Chem.* **2005**, *48*, 3221–3230.

(14) Cozza, G.; Bovini, P.; Zorzi, E.; Paletto, G.; Pagano, M. A.; Sarno, S.; Donella-Deana, A.; Zagotto, G.; Rosolen, A.; Pinna, L. A.; Meggio, F.; Moro, S. Identification of ellagic acid as potent inhibitor of protein kinase CK2: a successful example of a virtual screening application. *J. Med. Chem.* **2006**, *49*, 2363–2366.

(15) Pagano, M.A.; Paletto, G.; Di Maira, G.; Cozza, G.; Ruzzane, M.; Sarno, S.; Bain, J.; Elliott, M.; Moro, S.; Zagotto, G.; Meggio, F.; Pinna, L. A. Tetrabromocinnamic acid (TBCA) and related compounds represent a new class of specific protein kinase CK2 inhibitors. *ChemBioChem* **2007**, *8*, 129–139.

(16) Borges, F.; Roleira, F.; Milhazes, N.; Santana, L.; Uriarte, E. Simple coumarins and analogues in medicinal chemistry: Occurrence, synthesis and biological activity. *Curr. Med. Chem.* **2005**, *12*, 887–916.

(17) Lacy, A.; O'Kennedy, R. Studies on coumarins and coumarin-related compounds to determine their therapeutic role in the treatment of cancer. *Curr. Pharm. Des.* **2004**, *10*, 3797–3811.

(18) Åquist, J.; Medina, C.; Samuelsson, J.-E. A new method for predicting binding affinity in computer-aided drug design. *Protein Eng.* **1994**, *7*, 385–391.

(19) Bortolato, A.; Moro, S. In Silico binding free energy predictability by using linear interaction energy (LIE) method: Bromo-benzimidazole CK2 inhibitors as case study. *J. Chem. Inf. Model.* **2007**, *47*, 572–582.

(20) Hansson, T.; Åquist, J. Estimation of binding-free energies for HIV proteinase inhibitors by molecular dynamics simulation. *Protein Eng.* **1995**, *8*, 1137–1144.

(21) Graffner-Nordberg, M.; Kolmodin, K.; Aqvist, J.; Queener, S. F.; Hallberg, A. Design, synthesis, computational prediction, and biological evaluation of ester soft drugs as inhibitors of dihydrofolate reductase from *Pneumocystis carinii. J. Med. Chem.* **2001**, *44*, 2391–2402.

(22) Huang, D.; Caflisch, A. Efficient evaluation of binding free energy using continuum electrostatics solvation. *J. Med. Chem.* **2004**, *47*, 5791–5797.

(23) Zhou, R.; Friesner, R. A.; Ghoshs, A.; Rizzo, R. C.; Jorgensen, W. J.; Levy, R. M. New linear interaction method for binding affinity calculations using a continuum solvent model. *J. Phys. Chem. B* **2001**, *105*, 10388–10397.

(24) Tounge, B. A.; Reynolds, C. H. Calculation of the binding affinity of β-secretase inhibitors using the linear interaction energy method. *J. Med. Chem.* **2003**, *46*, 2074–2082.

(25) Singh, P.; Mhaka, A. M.; Christensen, S. B.; Gray, J. J.; Denmeade, S. R.; Isaacs, J. T. Applying linear interaction energy method for rational design of noncompetitive allosteric inhibitors of the sarco- and endoplasmic reticulum calcium-ATPase. *J. Med. Chem.* **2005**, *48*, 3005–3014.

(26) Ermakova, I.; Boldyreff, B.; Issinger, O. G.; Niefind, K. Crystal structure of a C-terminal deletion mutant of human protein kinase CK2 catalytic subunit. *J. Mol. Biol.* **2003**, *330*, 925–934.

(27) Niefind, K.; Guerra, B.; Ermakowa, I.; Issinger, O. G. Crystal structure of human protein kinase CK2: insights into basic properties of the CK2 holoenzyme. *EMBO J.* **2001**, *20*, 5320–5331.

(28) Niefind, K.; Guerra, B.; Pinna, L. A.; Issinger, O. G.; Schomburg, D. Crystal structure of the catalytic subunit of protein kinase CK2 from Zea mays at 2.1 A resolution. *EMBO J.* **1998**, *17*, 2451–2462.

(29) Pechkova, E.; Zanotti, G.; Nicolini, C. Three-dimensional atomic structure of a catalytic subunit mutant of human protein kinase CK2. *Acta Crystallogr. Sect. D: Biol. Crystallogr.* **2003**, *59*, 2133–2139.

(30) Battistutta, R.; Mazzorana, M.; Cendron, L.; Bortolato, A.; Sarno, S.; Kazimierczuk, Z.; Canotti, G.; Moro, S.; Pinna, L. A. Role of water and a positive electrostatic potential in the binding of protein kinase CK2 inhibitors. *ChemBioChem* **2007**, *8*, 1804–1809.

(31) ACD/pK$_a$, version 10.0, Advanced Chemistry Development, Inc., Toronto ON, Canada, www.acdlabs.com, 2006.

(32) Battistutta, R.; De Molier, E.; Sarno, S.; Zanotti, G.; Pinna, L. A. Structural features underlying selective inhibition of protein kinase CK2 by ATP site-directed tetrabromo-2-benzotriazole. *Protein Sci.* **2001**, *10*, 2200–2206.

(33) Meggio, F.; Shugar, D.; Pinna, L. A. Ribofuranosyl-benzimidazole derivatives as inhibitors of casein kinase-2 and casein kinase-1. *Eur. J. Biochem.* **1990**, *187*, 89–94.

(34) Battistutta, R.; De Moliner, E.; Sarno, S.; Zanotti, G.; and Pinna, L. A. *Protein Sci.* **2001**, *10*, 2200–2206.

(35) Leslie, A. G. W. In *Crystallographic Computing V*; Moras, D., Podjarny, A. D., Thierry, J. P., Eds.; Oxford University Press, Oxford, U.K., 1991; pp 27–38.

(36) Collaborative Computational Project, Number 4, The *CCP*4 suite: Programs for protein crystallography. *Acta Crystallogr.* **1994**, *D50*, 760–763.

(37) Lovell, S. C.; Davis, I. W.; Arendall, W. B., 3rd; de Bakker, P. I.; Word, J. M.; Prisant, M. G.; Richardson, J. S.; Richardson, D. C. Structure validation by C-alpha Geometry: phi, psi and C-beta deviation. *Proteins: Struct., Funct., Genet.* **2003**, *50*, 437–450.

(38) Emsley, P.; Cowtan, K. Coot: Model-building tools for molecular graphics. *Acta Crystallogr.* **2004**, *D60*, 2126–2132.

(39) Meggio, F.; Donella Deana, A.; Pinna, L. Endogenous phosphate acceptor proteins for rat liver cytosolic casein kinases. *J. Biol. Chem.* **1981**, *256*, 11958–11961.

(40) Sarno, S.; Vaglio, P.; Meggio, F.; Issinger, O.-G.; Pinna, L. A. Protein kinase CK2 mutants defective in substrate recognition. Purification and kinetic analysis. *J. Biol. Chem.* **1996**, *271*, 10595–10601.

(41) MOE (The Molecular Operating Environment), version 2006.08, software available from Chemical Computing Group Inc., 1010 Sherbrooke Street West, Suite 910, Montreal, Canada H3A 2R7; http://www.chemcomp.com.

(42) Cornell, W. D.; Cieplak, P.; Bayly, C. I.; Gould, I. R.; Merz, K. M.; Ferguson, D. M.; Spellmeyer, D. C.; Fox, T.; Caldwell, J. W.; Kollman, P. A. A second generation force field for the simulation of proteins, nucleic acids and organic molecules. *J. Am. Chem. Soc.* **1995**, *117*, 5179–5196.

(43) Halgren, T. Merck molecular force field. I. Basis, form, scope, parameterization, and performance of MMFF94. *J. Comput. Chem.* **1996**, *17*, 490–519.

(44) Carlson, A.; Jorgensen, W, L. An extended linear response method for determining free energies of hydration heather. *J. Phys. Chem.* **1995**, *99*, 10667–10673.

(45) Gallicchio, E.; Zhang, L. Y.; Levy, R. M. The SGB/NP hydration free energy model based on the surface generalized born solvent reaction field and novel nonpolar hydration free energy estimators. *J. Comput. Chem.* **2002**, *23*, 517–529.